Journal of Materials Chemistry

Cite this: *J. Mater. Chem.*, 2012, **22**, 1613

www.rsc.org/materials

PAPER

Role of pH and temperature on silica network formation and calcium incorporation into sol–gel derived bioactive glasses

Esther M. Valliant,[a] Claudia A. Turdean-Ionescu,[b] John V. Hanna,[b] Mark E. Smith[b] and Julian R. Jones*[a]

Received 11th July 2011, Accepted 14th November 2011
DOI: 10.1039/c1jm13225c

Bioactive glasses and inorganic/organic hybrids have great potential as implant materials. Bioactive glasses can bond to bone through the formation of a bone-like hydroxycarbonate apatite (HCA) layer and stimulate bone growth *via* their dissolution products. The brittle nature of these glasses can be combined with the toughness of a biodegradable polymer by forming a hybrid through the sol–gel process. However, for polymer incorporation, lower temperatures and milder pH conditions are required rather than the current method which uses pH < 1 and stabilisation at 600 °C. The impact of varying pH at low temperature processing (40 °C) on the inorganic component is unknown and must be investigated as a fundamental examination for hybrid research. This work seeks to combine pH control with a calcium source to examine the effect on porosity and silica network connectivity and to determine if raising the pH of synthesis can form a more highly connected glass without the need for high temperatures. Glass monoliths (70 mol% SiO_2 and 30 mol% CaO) were fabricated, using calcium hydroxide as the calcium precursor and at different pH values (pH 0.5–5.5). With a view to hybrid synthesis, gels were dried at 40 °C and were compared with glasses made from identical gels that had been stabilised at 600 °C. When dried at 40 °C, gels synthesised at pH < 2 were not mesoporous whereas those formed at pH > 2 were mesoporous. This indicates a difference in gel formation about the isoelectric point of silicic acid, which was confirmed by ^{29}Si solid state NMR. When immersed in simulated body fluid (SBF), the glasses stabilised at 600 °C were more porous, yet had a slower ion release rate than the gels dried at 40 °C. All gels and glasses formed an HCA layer in SBF; however, calcium was only incorporated into the silica network after stabilisation at 600 °C and thus a new way of incorporating calcium at low temperatures must still be found. This work is an important foundation for hybrid synthesis as raising the pH of the sol–gel process from pH < 1 to pH 5.5 was found to have no adverse effects on silica network formation and thus polymer can be incorporated into the sol–gel process at milder pH conditions without the concern of acid catalysed polymer degradation by chain scission.

Introduction

As the population ages, the prevalence of arthritis and other degenerative connective tissue diseases will increase. Currently, to repair a bone defect, a bone can be transplanted from the patient's hip area (iliac crest – autograft) or from another person (allograft). There is the risk of long term pain at the second surgery site with the former and infection with the latter.[1] These risks may be prevented by using a synthetic scaffold. A scaffold for bone tissue regeneration should bond to the existing bone, encourage cell attachment, have a porous structure suitable for cell ingrowth and degrade as new bone is formed.[2–4]

Bioactive glasses have proven bone bonding abilities. Bioglass® (45 wt% SiO_2, 24.5 wt% Na_2O, 24.5 wt% CaO, 6 wt% P_2O_5) was the first and it was formed through the melt derived method using high temperatures.[5] Bioglass® powders are currently used in orthopaedic surgery in non load-bearing applications.[6] Despite the favourable biological response, bioactive glasses are brittle and do not have the required mechanical properties for load bearing applications. Composites are alternative materials that can have increased toughness. HAPEX™ is a composite of hydroxyapatite incorporated into extruded polyethylene and can be shaped during surgery with a scalpel.[7] However, the majority of the bioactive particles are masked by the polymer and cells attached preferentially to the bioactive particles. Combining a polymer and glass at a finer scale may allow for improved cellular response and improved mechanical properties.[8] Hybrids comprised of inorganic and organic species that interact at the molecular level, and are

[a]*Department of Materials, Imperial College London, South Kensington, UK. E-mail: julian.r.jones@imperial.ac.uk*
[b]*Department of Physics, University of Warwick, Coventry, UK*

indistinguishable above the submicron scale, have the potential to overcome this problem.[9] There is also potential to gain fine control over their mechanical properties and degradation rates to produce materials with congruent degradation profiles.[10]

The sol–gel process is a low temperature process that has been used to synthesise bioactive glasses, such as 70S30C (70 mol% SiO_2, 30 mol% CaO).[11,12] Hydrolysis of the alkoxysilane groups is followed by condensation to form the glass network.[13,14]

Hydrolysis:

$$Si(OR)_4 + n\ H_2O \rightarrow (OH)_nSi(OR)_{4-n} + n\ ROH$$

Condensation:

$$2\ Si(OH)_4 \rightarrow (OH)_3Si{-}O{-}Si(OH)_3 + H_2O$$

A hybrid material can be formed by introducing a polymer into the sol–gel process,[15] where the silica network can form around polymer chains. The silica network forms amongst the dissolved polymer, thus allowing the silica network and the polymer to interact at the molecular level.[8] The traditional sol–gel process uses an acid catalysed reaction (pH < 1) to form the silica network.[16] However this may be too acidic to incorporate a polymer directly into the sol–gel process, as the highly acidic conditions may cause polymer chain scission.

The time required for gelation of the silica sol–gel process is dependent on the pH. Gelation is slowest at pH 2 (the isoelectric point of silicic acid) as the gelation can be catalysed when the silica species are in the protonated or anionic form.[17] These two catalysis methods follow slightly different pathways. It has been proposed that in acidic conditions (pH < 2), the hydrolysis of the first alkoxy silane group is rapid, but each successive hydrolysis is slower; whereas for silica in the anion form (pH > 2), the initial hydrolysis is very slow, but the process continues and condenses rapidly. The effect of pH on the silica structure, porosity and bioactivity of 70S30C is unknown and will be examined here.

Calcium is an important component of bioactive glasses, and in the sol–gel process, it produces mesoporous glasses and this porosity has a great effect on the rate of dissolution and thus the bioactivity of the glass.[2] Pore size has been controlled by calcium content,[20] sintering temperature[2] and pore seeding with trimethylethoxysilane.[21] The role of synthesis pH on mesoporosity is unknown.

A soluble calcium source is required to incorporate calcium into the sol–gel process. However, commonly used calcium precursors have limitations in terms of calcium incorporation. Calcium chloride simply recrystallises on the surface of hybrid materials during drying.[15] Calcium nitrate is a common calcium precursor in the sol–gel process as it is highly soluble in the sol. Traditional 70S30C glasses using calcium nitrate tetrahydrate require heating to 600 °C to remove toxic nitrates from the glass, which is too high for polymer incorporation.[11] Lin *et al.* showed that Ca^{2+} from calcium nitrate is not incorporated into the silicate network until the stabilisation temperature, *i.e.* above 400 °C.[18] This has been shown to cause inhomogeneity in sol–gel glasses, even though stabilised at high temperature.[19] Hence, for hybrid formation at low temperatures, these existing calcium sources are not suitable.

The aim of this study was to form a calcium containing silica glass while varying the pH of the sol–gel condensation step to determine the effect on mesoporosity and silica network connectivity. Raising the pH could be used to encourage the condensation of the silica network and possibly even incorporate calcium without the use of high temperatures.

Results and discussion

Composition testing

Sol–gel gels and glasses were successfully formed for a synthesis pH between 0.5 and 5.5 and were then dried at 40 °C or stabilised at 600 °C. The composition of the gels and glasses, as confirmed by lithium metaborate fusion, was 70 ± 4 mol% SiO_2 and 30 ± 4 mol% CaO.

Mesoporosity characterisation

In the sol–gel process, nanoparticles of silica form during the condensation step. These primary particles agglomerate into a gel at room temperature and then continue to fuse together during the drying process, and as the temperature increases to 600 °C, they form quarternary particles. The spaces between the particles make the glasses mesoporous.[18] When calcium is present in the sol–gel process, its positive charge affects the way the particles agglomerate, thus changing the mesoporous structure of the glass.

All synthesised glasses were found to be mesoporous, except for gels synthesised at pH < 2 and dried at 40 °C. This threshold corresponds to the isoelectric point of silicic acid, pH 2. Pore size

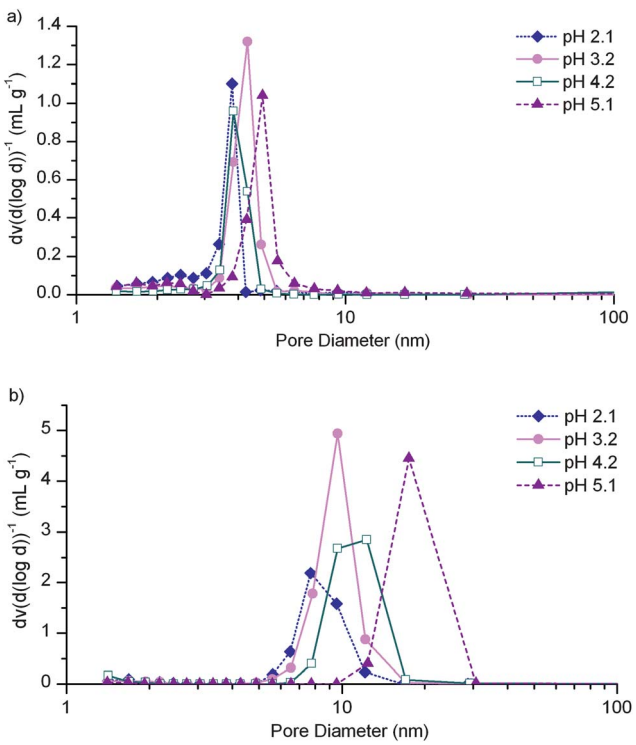

Fig. 1 Pore size distribution over a range of sol pH for a) gels dried at 40 °C and b) glasses stabilised at 600 °C.

distributions were obtained using nitrogen sorption Barrett-Joyner-Halenda (BJH)[22] correlation (Fig. 1).

For glasses stabilised at 600 °C, the modal pore diameter increased as pH increased (Fig. 1b), from 8 nm at pH 2.1 to 18 nm at pH 5.1. Gels dried at 40 °C had a fairly consistent modal pore diameter of 3–6 nm when synthesised with a sol pH > 2 (Fig. 1a). The gels synthesised with pH < 2 and dried at 40 °C were not mesoporous. The distributions were narrower for gels dried at 40 °C than for those stabilised at 600 °C, and the glasses at high temperature absorbed more nitrogen and thus had greater porosity.

All gels and glasses that were mesoporous produced Type IV nitrogen sorption isotherms according to IUPAC classification[23] (Fig. 2). All gels synthesised at pH > 2 and dried at 40 °C had H2 hysteresis loops,[23] with a positively sloped absorption in advance of the hysteresis loop (Fig. 2a).

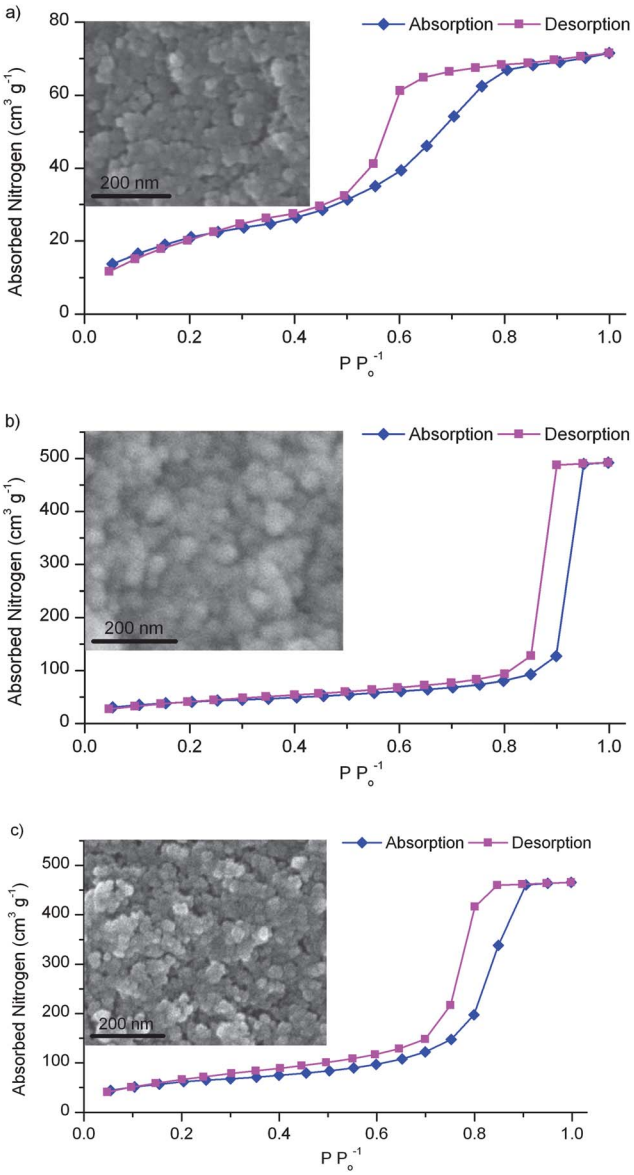

Fig. 2 Isotherm and SEM image of 70S30C a) gel formed at pH 5.1 and dried at 40 °C, b) glass formed at pH 5.1 stabilised at 600 °C and c) glass formed at pH 3.1 stabilised at 600 °C.

This is said to be an indication of pores having an 'ink bottle' shape with pore throats being narrower than their diameter.[23] However, SEM showed rounded and slightly agglomerated particles (25–35 nm). The shape of the nitrogen isotherm varied with pH for the glasses stabilised at 600 °C. In Fig. 2b, the glass synthesised at pH 5.1 had an H1 hysteresis loop, which is an indication of pores between uniform closely packed spherical particles[23] and was confirmed by SEM (diameter 50 nm). As the synthesis pH decreased (pH < 5), an H2 hysteresis loop developed which is characteristic of 'ink bottle' shaped pores.

The isotherm of the glass synthesised at pH 3.1 is typical (Fig. 2b) of Type H2 hysteresis but the particles were less well defined in SEM (diameter 35 nm). Thus the sol pH had an effect on both the modal pore size, pore shape and topography of the glass when stabilised at 600 °C.

The surface area was related to the modal pore diameter (Fig. 3). The pore size of the gels dried at 40 °C increased slightly as the sol pH increased. Surface area was expected to decrease as the pore size increased but remained fairly constant. If the total porosity remains constant, then several smaller pores have been replaced with fewer larger pores, resulting in a smaller surface area. In this case, the pore size increased without a corresponding reduction in surface area, implying that the number of pores has only reduced slightly. This increase in pore size was also noted visually as the opacity of the gels increased with pH, such that the gels at pH 4.7 looked and felt similar to glasses dried at 600 °C, due to lower water content and greater light diffraction from the larger pores.

The glasses stabilised at 600 °C follow a trend that can be described in two parts. For pH ≤3, the pore size remained constant (12 nm) but the surface area increased (98 to 216 m^2 g^{-1}) as pH increased from 1.4 to 3.2. This implies that the number of pores and the total porosity of the material increased. As the pH increased from 3.2 to 5.1, the pore size increased (12 to 30 nm) and the surface area decreased (216 to 145 m^2 g^{-1}), as many small pores were replaced with fewer larger pores, resulting in a lower surface area.

For glass synthesis at a pH below the isoelectric point (pH 2), the silica groups were protonated and thus the sol–gel process was acid catalysed; whereas above pH 2, the mechanism changed as the silica species were anionic. The lack of mesoporosity in gels dried at 40 °C, following sol production at pH < 2, could be an

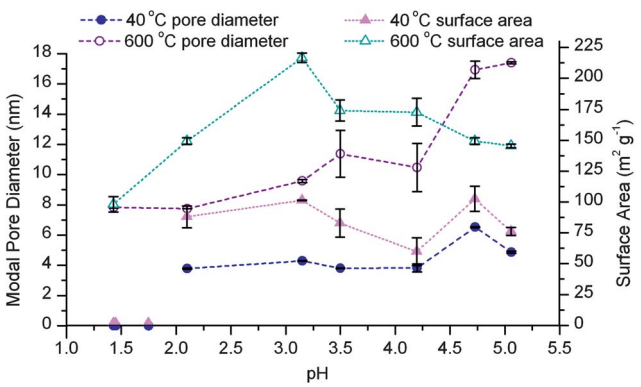

Fig. 3 Dependence of surface area and pore size on pH determined using nitrogen sorption for gels dried at 40 °C and glasses stabilised at 600 °C.

indication of poorer network formation. Thus the porosity measurements suggest that the conventional acid catalysed sol–gel process (pH < 1) does not create a mesoporous network at low temperature conditions, but pH > 2 did. So there are no adverse effects and potential beneficial effects on the silica network by raising the pH of the sol–gel synthesis. However, the more neutral pH conditions offer some exciting opportunities for hybrid development as such synthesis is compatible with polymer incorporation directly into the sol–gel process.

NMR of the silicate network

Synthesis pH did affect the silica network and the formation of bridging oxygen bonds when examined using solid state ^{29}Si NMR (Fig. 4). There appears to be a change in the NMR spectra about the isoelectric point (pH 2) which is consistent with the mesoporosity data. All gels dried at 40 °C had a greater proportion of Q^3 and Q^4 species than the glasses stabilised at 600 °C (Table 1). A Q^n species is a Si–O tetrahedron with n bridging oxygen bonds to other tetrahedra in the silica glass network (as illustrated in the insets in Fig. 4). The reduction in network connectivity (increase in the amount of lower Q^n species) noted in glasses at 600 °C shows that the silica network has fewer bridging oxygen bonds. This indicates that high temperature led to more successful incorporation of calcium into the glass network, where calcium ions (Ca^{2+}) coordinate to silicate groups ($Si–O^-$) resulting in the corresponding disruption of the silicate network. This is supported by the increase in Q^1 and Q^2 species. Lin *et al.* found that calcium did not incorporate into the silica network until 450 °C for 70S30C glasses formed at pH < 1,[18] and the data in Table 1 shows this is true up until pH 5.5. Thus there is no detrimental effect, or change in behaviour in the glass by raising the synthesis pH.

The ^{29}Si MAS NMR suggests that all gels dried at 40 °C have very similar network connectivity (Q^n) distribution, at the most local level, despite the very different reaction rates. Glasses synthesised at pH < 2 took up to a day to gel whereas for glasses synthesised at pH > 2, an increase in pH increased the rate of gelation. Gelation at pH 3 took 10 min, pH 4.5 took 5 min and pH 5.1 took 30 s. The gelation rates appear to have some effect on the degree of order in the network. For a dilute spin-$^1/_2$ nucleus (such as ^{29}Si in this material), the residual linewidth under magic angle spinning is dominated by the range of isotropic chemical shifts which is termed chemical shift dispersion.[24] This means that the samples that gelled faster show more disorder as indicated by the greater linewidth. This increase in linewidth for samples gelled at higher pH can be gauged by the relative resolution of the Q^3 given its shift position does not change (Fig. 4, Table 1). Although this is not definitive evidence, it is certainly consistent with the potential greater disorder created by porosity, although the length scales are very different.

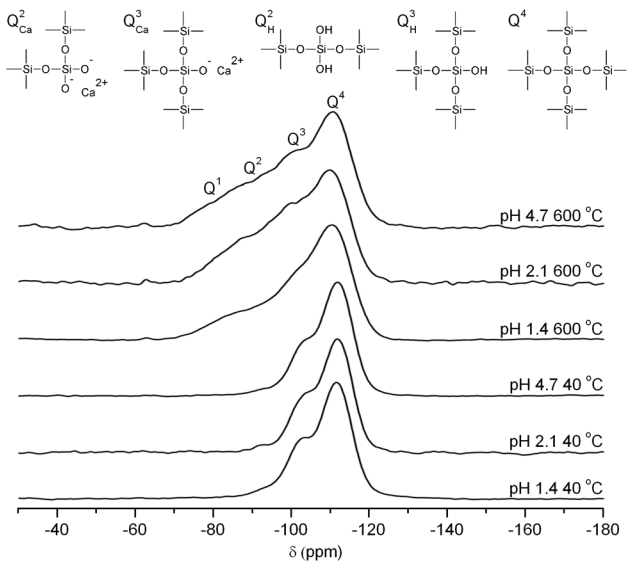

Fig. 4 ^{29}Si MAS NMR showing the silica speciation of the network for gels dried at 40 °C and glasses stabilised at 600 °C.

The gelation rate also had an impact on the macrostructure of the glasses. The faster-gelling samples dried at 40 °C and formed at pH > 2, were found to have a mesoporous network as confirmed by nitrogen sorption. However, NMR indicates that the silica network was formed, but that calcium was not incorporated at 40 °C. This further reinforces the findings by Lin *et al.* that calcium nitrate is not a suitable calcium precursor at low temperatures as the calcium does not enter the silica network and should not be used when seeking polymer incorporation.[18] For the glasses stabilised at 600 °C with a synthesis pH of 4.7, the concentration of Q^4 species was higher while the concentration of lower Q species (*i.e.* with Ca^{2+} or H^+ charge compensating the non-bridging oxygens) was lower than at pH 2.1 (Table 1). This might suggest that at high pH, less calcium was incorporated in the silicate network, possibly due to the rapid and complete condensation of the silica network catalysed by the elevated pH causing the calcium to less readily enter the network.

Bioactivity testing

Gels and glasses synthesised at three pH conditions were chosen for bioactivity testing as they represented acid catalysed reaction (pH 1.7), gelation near the isoelectric point (pH 2.1) and anionic sol–gel reaction (pH 4.7). The stabilised glasses (600 °C) had different ion concentration profiles compared to the gels dried at 40 °C (Fig. 5). For gels dried at 40 °C, sol pH had no effect on the ion concentrations in solution. There was fast dissolution of the gel, as shown by the release of ~60 μg mL^{-1} of Si by 24 h and an initial spike in the Ca concentration (8 h). This was followed by a decrease in the calcium concentration and the phosphorus concentration approaching 0 after 24 h, which suggests the formation of HCA. HCA formation was confirmed with FTIR and XRD (Fig. 6 and 7). Thus the gels are very bioactive as they can form HCA so quickly. The NMR showed a more highly connected network for the gels dried at 40 °C than the glasses stabilised at 600 °C; however, the dissolution indicates that the glass network is more resistant to dissolution at 600 °C despite the lower Q^n speciation. This might indeed be the case as effective ionic cross-linking by calcium could produce a stronger network.

The concentrations of calcium and phosphorus in SBF solution followed similar trends in the glasses stabilised at 600 °C for all sol pH values. However the rate of silica release was slowest at the highest pH value (4.7), suggesting that a more durable network was formed at higher pH values. The slow silica release

Table 1 ^{29}Si NMR showing the silica speciation as a relative intensity (I) for gels dried at 40 °C and glasses stabilised at 600 °C where average errors are ±1 ppm for the chemical shift (δ) and for I ± 2% for samples heated to 40 °C and ±4% for samples heated to 600 °C

	Q^1		Q^2		Q^3		Q^4	
Sample	δ (ppm)	I (%)	δ (ppm)	I (%)	δ (ppm)	I (%)	δ (ppm)	I (%)
pH 1.4 40 °C	—	—	−93.4	4	−102.1	26	−111.6	70
pH 2.1 40 °C	—	—	−92.3	3	−102.8	31	−111.9	66
pH 4.7 40 °C	—	—	−93.3	4	−102.9	28	−111.9	68
pH 1.4 600 °C	−80.9	8	−88.6	14	−99.4	34	−110.5	44
pH 2.1 600 °C	−78.6	7	−89.8	24	−100.7	24	−111.2	45
pH 4.7 600 °C	−78.8	4	−89.2	19	−101.3	26	−111.0	51

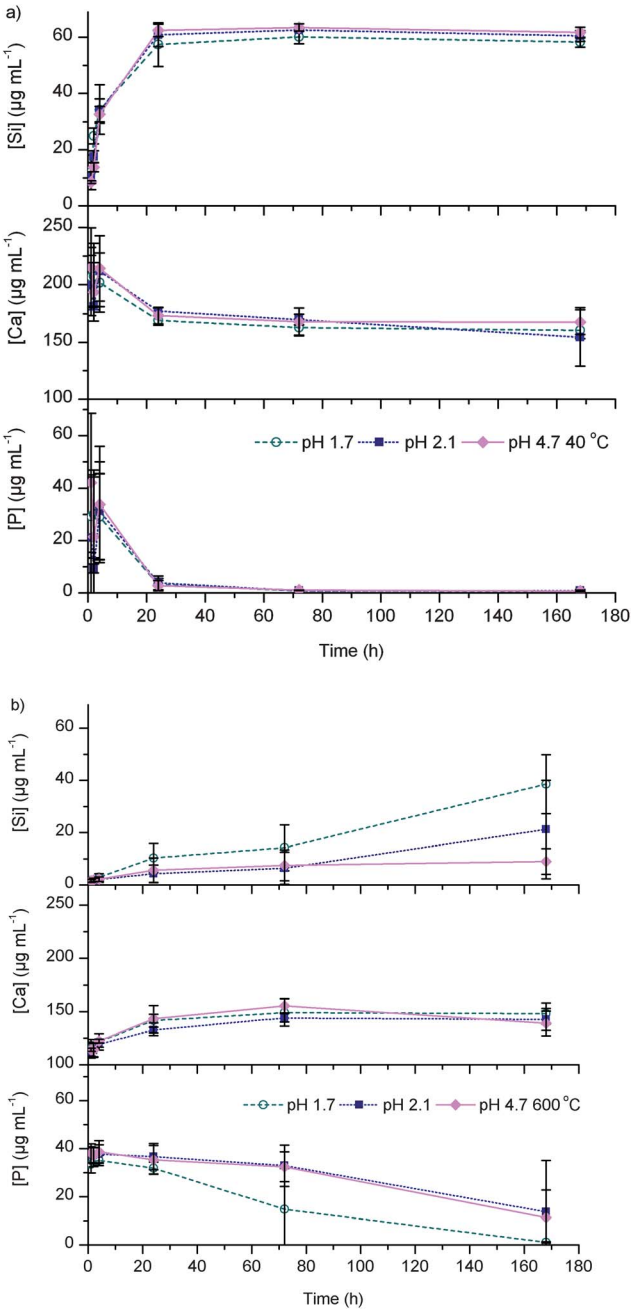

Fig. 5 Ion release profiles with varying sol pH of 70S30C a) gels dried at 40 °C and b) glasses stabilised at 600 °C.

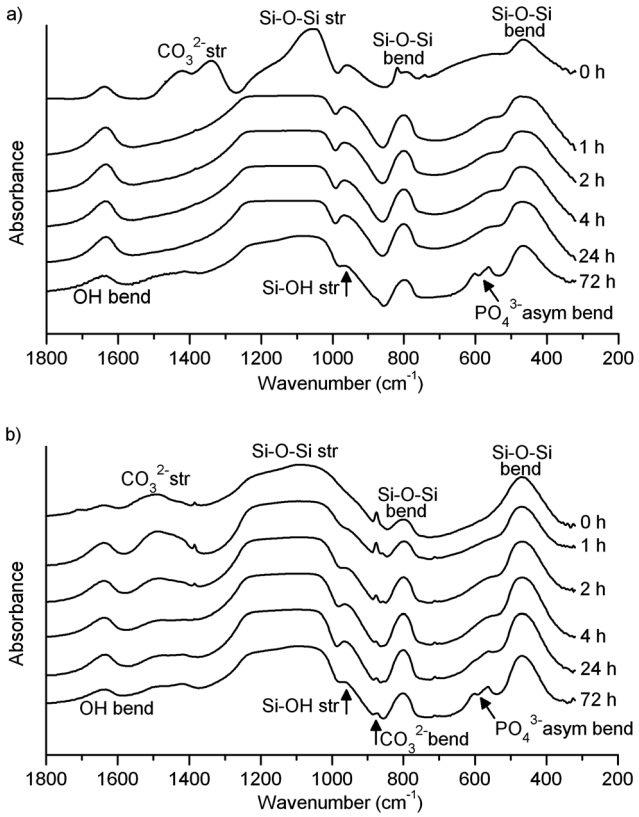

Fig. 6 FTIR after SBF immersion from 1 to 72 h at synthesis pH 4.7 a) for gels dried at 40 °C and b) glasses stabilised at 600 °C.

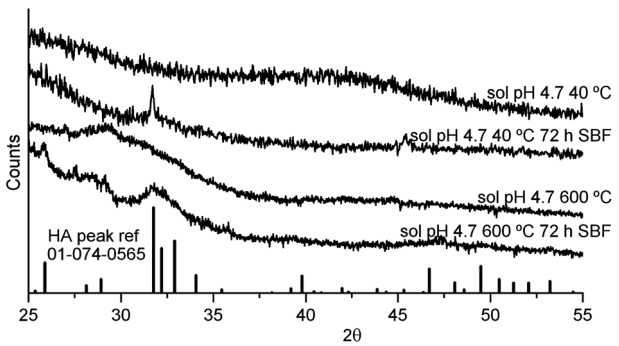

Fig. 7 XRD following SBF immersion for 72 h at synthesis pH 4.7 for gels at 40 °C and glasses stabilised at 600 °C.

at the highest synthesis pH indicates that the less acidic sol–gel formation route was beneficial and is preferred to the conventional low pH (pH < 1) sol–gel route.

The ion concentration profiles at low temperatures are the same for all of the synthesis pH values. This is consistent with the similar NMR results which showed greater differences due to drying temperature than synthesis pH. In the case of the gels dried at 40 °C, the similar local network connectivity over all pH values resulted in similar dissolution profiles, despite the significant differences in porosity, indicating that the local structure is more important than the macroscopic property.

Glass stabilisation at 600 °C resulted in much lower Si and Ca dissolution than from gels dried at 40 °C, indicating a reduction in bioactivity due to a stronger network. However after immersion in SBF, all gels and glasses were found to form HCA within 72 h, as shown by FTIR and confirmed with XRD (Fig. 6 and 7). All glasses had a sharp band in the FTIR spectra at 950 cm^{-1}, which corresponds to the Si–OH bond,[25] due to mobile protons forming surface hydroxyl groups in the aqueous process. This is consistent with the NMR which shows that the Q^3 species are a major part of the silica network (26–34%). The NMR also showed that the gels dried at 40 °C had a more highly connected structure, yet faster silicon release rate in SBF. The samples dried at 40 °C have much higher Si–OH content which probably aids dissolution. Through stabilisation, it is possible that some of the chains changed their configuration to three- or four-membered rings[26] and this can explain the lower dissolution rates for silicon in these samples. The silicon atoms in these rings are probably connected to Ca^{2+} cations as in Q^2 and Q^3. If Q^4 species were present in the ring, a shoulder in the ^{29}Si NMR at around −107 ppm would be expected.[26] However, the linewidths of all Q^n species (n = 2–4) (not shown in the Table 1, but can be very clearly seen in Fig. 4) increase substantially compared with those in xerogel samples, suggesting more disorder in the tetrahedral network and further support for calcium incorporation.

Conclusions

Sol–gel glasses with a composition of 70 mol% SiO_2 and 30 mol% CaO were successfully synthesised with sols over a pH range of 0.5 to 5.5. Raising the synthesis pH resulted in larger pores when stabilised at 600 °C and mesoporous gels for pH > 2 when dried at 40 °C. All gels dried at 40 °C had faster ion release upon immersion in SBF than glasses stabilised at 600 °C, which suggests that the higher temperatures created more durable glasses. Also calcium was only in the silica network for glasses at 600 °C and drying at low temperatures (40 °C) over the range of pH synthesis was not able to incorporate calcium. Varying the pH is a new method to change the pore size of a glass stabilised at 600 °C and raising the synthesis pH did not have an adverse effect to the silica network at low temperatures. This lays a foundation for the creation of hybrids through the sol–gel route. A new method for calcium incorporation is still required, but this has shown that the conventional highly acidic conditions (pH < 1) of the sol–gel reaction are not required, and it is possible to raise the pH of synthesis to milder conditions which will protect the polymer from chain scission reactions.

Experimental

Materials

Tetraethyl orthosilicate (TEOS), calcium hydroxide ($Ca(OH)_2$) and concentrated nitric acid were all purchased from Sigma-Aldrich Company Ltd (Dorset, UK). Sample moulds by Nalgene (60 mL polymethylpentene (PMP) moulds with polypropylene (PP) lids) were also purchased from Sigma.

Preparation of elevated pH 70S30C sol–gel glasses with calcium hydroxide

Sol–gel gels and glasses (70 mol% SiO_2 and 30 mol% CaO) were synthesised from a range of sols with pH between 0.5 and 5.5, followed by ageing and drying of gels at 40 °C and the glasses were further stabilised at 600 °C (Fig. 8). The silica precursor of 16.7 mol% TEOS was hydrolysed in 0.028 M HNO_3 for 1 h. The calcium precursor combined at a 1 : 2 molar ratio of concentrated HNO_3 to a slurry of 36.7 wt% $Ca(OH)_2$. The pH was adjusted between pH 3 and 10. The silica and calcium precursor solutions were combined in a 2 : 1 volume ratio. The pH of the final 70 mol% Si and 30 mol% Ca sol was measured and was then poured into moulds and sealed. All samples were aged for 3 days at 40 °C before drying at a low (40 °C, 5 days) or high temperature stabilisation (600 °C). To stabilise, the samples were heated for 20 h at 60 °C (0.1 °C min^{-1}), 24 h at 90 °C followed by 130 °C and held for 20 h followed by cooling to room temperature. The temperature was then raised by 1 °C min^{-1} to 300 °C and held for 3 h followed by 5 h at 600 °C.

Glass characterisation

XRD. X-ray diffraction was performed on a Philips PW1700 Automated Powder Diffractometer. The radiation source was Cu Kalpha at 40 KV/40 mA with a secondary graphite crystal monochromater. The sample was ground and placed on an amorphous silicon disk. The diffraction was measured between 25 and 55° 2θ, with a 0.02° step size and a counting time of 30 s at each step.

SEM. Scanning electron microscopy was performed on a Leo 1525 with Gemini column fitted with a gun voltage of 5 kV upon glass fracture surfaces coated with chromium.

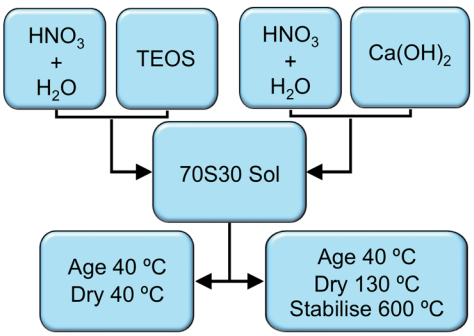

Fig. 8 Schematic for the formation of elevated pH 70S30C sol–gel glasses.

Nitrogen sorption

Mesoporosity was determined by nitrogen sorption using a Quantachrome Autosorb 6B, Model AS6 KR. Glasses were degassed >16 h with a Quantachrome Autosorb degasser Model AD4. The Brunauer-Emmett-Teller (BET) method was used to determine the surface area of the material[23] and the Barrett-Joyner-Halenda (BJH) method was applied to the desorption isotherm to determine the pore size distribution.[22] Both the surface area and modal pore size distribution measurements were repeated in triplicate. The mean values and standard deviation are reported.

^{29}Si MAS NMR spectroscopy

^{29}Si Magic Angle Spinning Nuclear Magnetic Resonance (MAS NMR) spectra were collected on a Varian InfinityPlus 300 MHz spectrometer operating at 59.62 MHz. A 5.0 μs (45° tip angle) pulse and 20 s recycle delays have been used to produce relaxed spectra. The spectra were referenced to TMS at 0 ppm.

SBF test

Apatite formation in simulated body fluid (SBF) was tested by immersing the sol–gel glasses to examine the dissolution profile and the formation of hydroxycarbonate apatite (HCA) on the surface of the material.

The SBF was formed by the following method as described by Kokubo and Takadama.[27] Each sample was measured in triplicate, where 75 mg of glass was immersed in 50 mL of SBF and mixed at 120 rpm in an orbital shaker held at 37 °C for 1, 2, 4, 24, 72 and 168 h. The solids were collected with filter paper (particle retention 5–13 μm) washed with acetone and dried overnight at 40 °C.

The solids were then examined by Fourier transform infrared spectroscopy (FTIR) and X-ray diffraction (XRD) and the solutions were analysed by inductively coupled plasma spectroscopy (ICP). Transmission FTIR was measured from potassium bromide pellets with a Bruker Vector 22 thermal gravimetric-infrared spectrometer (TGA-IR). A Thermo Scientific iCAP 6300 Duo inductively coupled plasma–optical emission spectrometer (ICP-OES) with auto sampler was used to determine the Si, P and Ca concentrations.

Acknowledgements

This research has been funded in part by the Natural Sciences and Engineering Research Council of Canada (NSERC), Canadian Centennial Scholarship Fund UK, the Department of Materials, Imperial College London, the EPSRC (EP/E057098/1 and EP/E051669) and the Philip Leverhulme Prize. The NMR equipment used in this research received funding from EPSRC, BBSRC, the University of Warwick and Birmingham Science City Projects supported by Advantage West Midlands and the European Regional Development Fund.

References

1 R. C. Sasso, J. C. LeHuec, C. Shaffrey and the Spine Interbody Research Group, *J. Spinal Disord. Tech.*, 2005, **18**, S77–S81.
2 J. R. Jones, *J. Eur. Ceram. Soc.*, 2009, **29**, 1275–1281.
3 O. Mahony and J. R. Jones, *Nanomedicine*, 2008, **3**, 233–245.
4 P. Ducheyne and Q. Qiu, *Biomaterials*, 1999, **20**, 2287–2303.
5 L. L. Hench, R. J. Splinter, W. C. Allen and T. K. Greenlee, *J. Biomed. Mater. Res.*, 1971, **5**, 117–141.
6 L. L. Hench, *J. Mater. Sci.: Mater. Med.*, 2006, **17**, 967.
7 M. J. Dalby, M. V. Kayser, W. Bonfield and L. Di Silvio, *Biomaterials*, 2002, **23**, 681–690.
8 B. Novak, *Adv. Mater.*, 1993, **5**, 422–433.
9 E. M. Valliant and J. R. Jones, *Soft Matter*, 2011, **7**, 5083–5095.
10 O. Mahony, O. Tsigkou, C. Ionescu, C. Minelli, L. Ling, R. Hanly, M. E. Smith, M. M. Stevens and J. R. Jones, *Adv. Funct. Mater.*, 2010, **20**, 3835–3845.
11 J. R. Jones, L. M. Ehrenfried and L. L. Hench, *Biomaterials*, 2006, **27**, 964–973.
12 S. Yue, P. D. Lee, G. Poologasundarampillai and J. R. Jones, *Acta Biomater.*, 2011, **7**, 2637–2643.
13 R. K. Iler, *J. Colloid Interface Sci.*, 1975, **53**, 476–488.
14 J. Wright and N. Sommerdijk, *Sol–gel Materials Chemistry and Applications*, Gordon and Breach Science Publishers, 2001.
15 G. Poologasundarampillai, C. Ionescu, O. Tsigkou, M. Murugesan, R. J. Hill, M. M. Stevens, J. V. Hanna, M. E. Smith and J. R. Jones, *J. Mater. Chem.*, 2010, **20**, 8952–8961.
16 P. Sepulveda, J. R. Jones and L. L. Hench, *J. Biomed. Mater. Res.*, 2002, **59**, 340–348.
17 R. K. Iler, in *The Chemistry of Silica*, John Wiley and Sons, Inc., New York, 1979, pp. 185–189, 209–213, 366–367.
18 S. Lin, C. Ionescu, K. J. Pike, M. E. Smith and J. R. Jones, *J. Mater. Chem.*, 2009, **19**, 1276–1282.
19 S. Lin, C. Ionescu, S. Baker, M. E. Smith and J. R. Jones, *J. Sol-Gel Sci. Technol.*, 2010, **53**, 255–262.
20 A. Martinez, I. Izquierdo-Barba and M. Vallet-Regí, *Chem. Mater.*, 2000, **12**, 3080–3088.
21 S. Lin, C. Ionescu, E. M. Valliant, J. V. Hanna, M. E. Smith and J. R. Jones, *J. Mater. Chem.*, 2010, **20**, 1489–1496.
22 Iupac, *Pure Appl. Chem.*, 1994, **66**, 1739–1758.
23 Iupac, *Pure Appl. Chem.*, 1985, **57**, 603–619.
24 K. J. D. MacKenzie and M. E. Smith, *Multinuclear Solid State NMR of Inorganic Materials*, Pergamon, Oxford, 2002.
25 H. Aguiar, J. Serra, P. González and B. León, *J. Non-Cryst. Solids*, 2009, **355**, 475–480.
26 C. J. Brinker, D. R. Tallant, E. P. Roth and C. S. Ashley, *J. Non-Cryst.Solids*, 1986, **82**, 117–126.
27 T. Kokubo and H. Takadama, *Biomaterials*, 2006, **27**, 2907–2915.